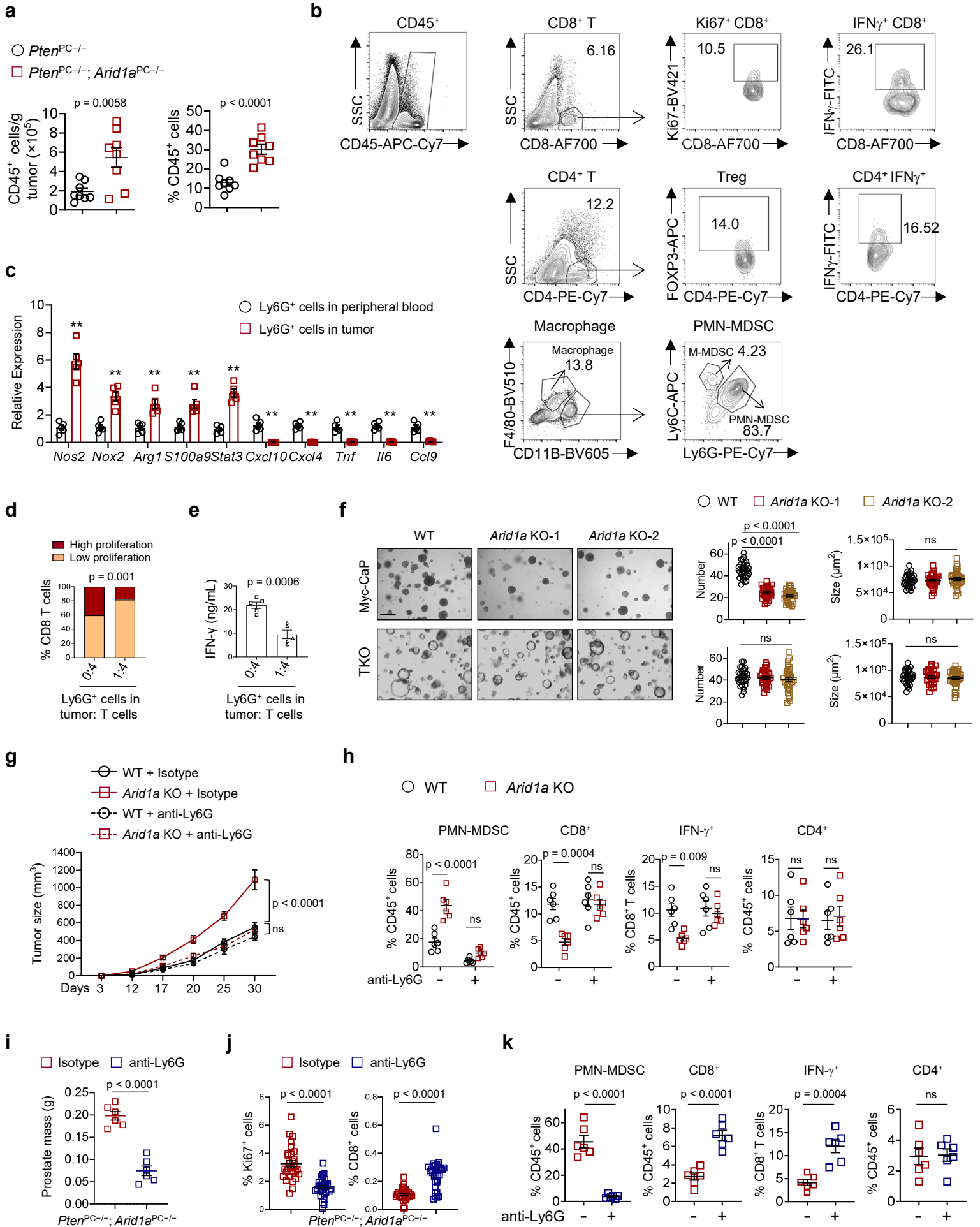
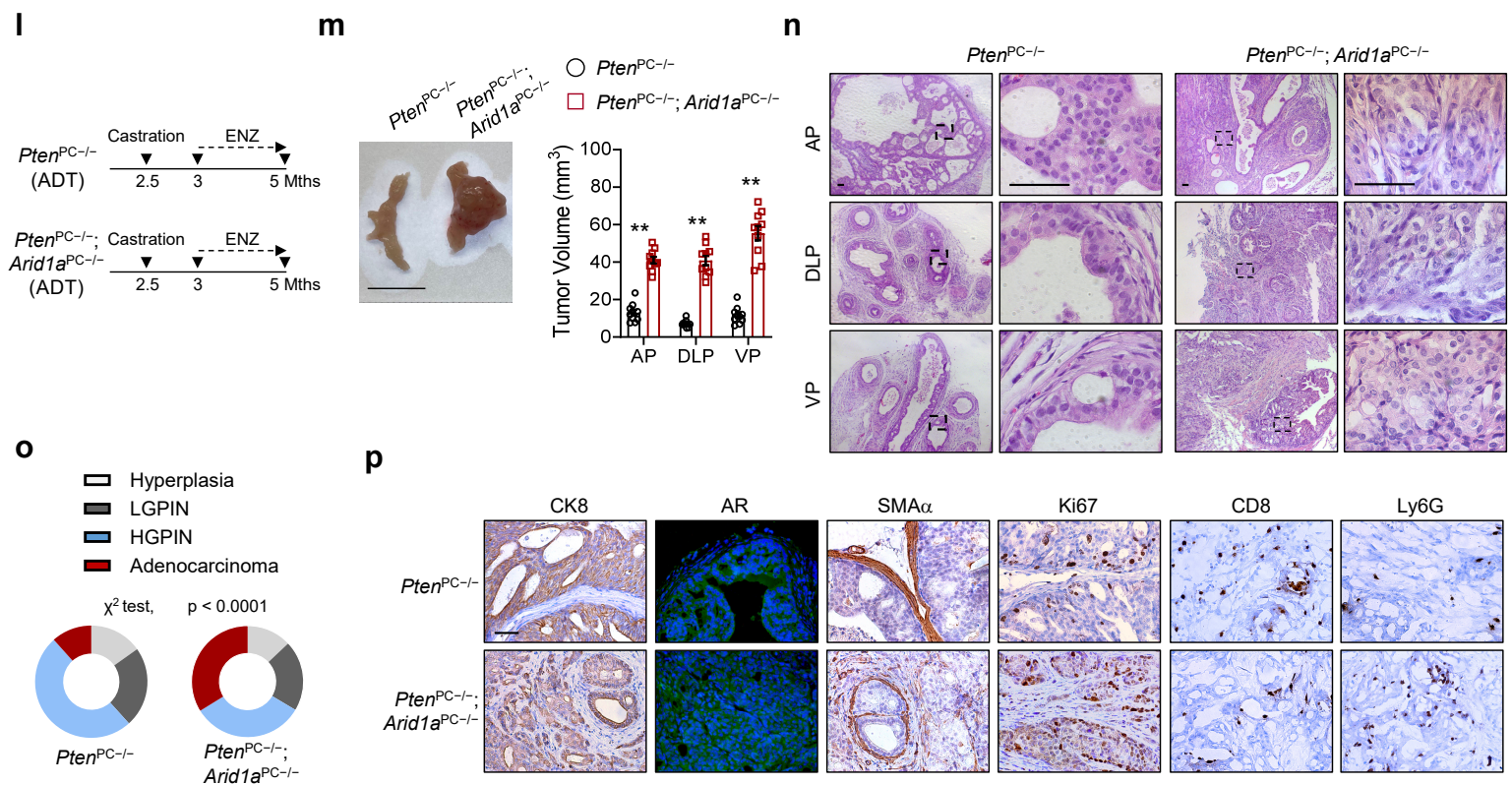


Supplementary Figure 1. *Arid1a* inactivation promotes prostate tumorigenesis.

a, ARID1A staining indexes using a 10-point quantification scale in cohorts of normal prostate tissues ($n = 40$) and tumors ($n = 100$). **b**, ARID1A expression levels stratified by PSA in TMA ($n = 100$). **c**, IHC score of ARID1A stratified by Gleason score (GS) in TMA ($n = 100$). **d**, ARID1A-stained sections of representative DLP and IB analysis of tissues from 6-month-old *Arid1a*^{flox/flox} and *Arid1a*^{PC-/-} mice ($n = 3$). Scale bar: 50 μ m. **e**, H&E-stained sections of representative AP, DLP, and VP in mice at 12 months of ages ($n = 10$, representative data are shown). Scale bar: 50 μ m. **f**, MRI analysis and quantitation of 16-week-old *Pten*^{PC-/-} and *Pten*^{PC-/-}; *Arid1a*^{PC-/-} prostates ($n = 10$). **g**, H&E-stained sections of 12-week-old *Pten*^{PC-/-} and *Pten*^{PC-/-}; *Arid1a*^{PC-/-} mice ($n = 15$, representative data are shown). Scale bars, 50 μ m. **h**, AR and CK8 staining of lymph nodes from 12-week-old mice. Scale bar, 50 μ m. **i**, Relative expression of lineage markers in epithelium from 12-week-old mouse prostates ($n = 3$), ns, no significance.

f, **i**, Data represent the mean \pm SEM. Statistical significance was determined by two-tailed χ^2 test (**a**, **b**, **c**) and two-tailed unpaired *t* test (**f**, **i**). Source data are provided as a Source Data file.

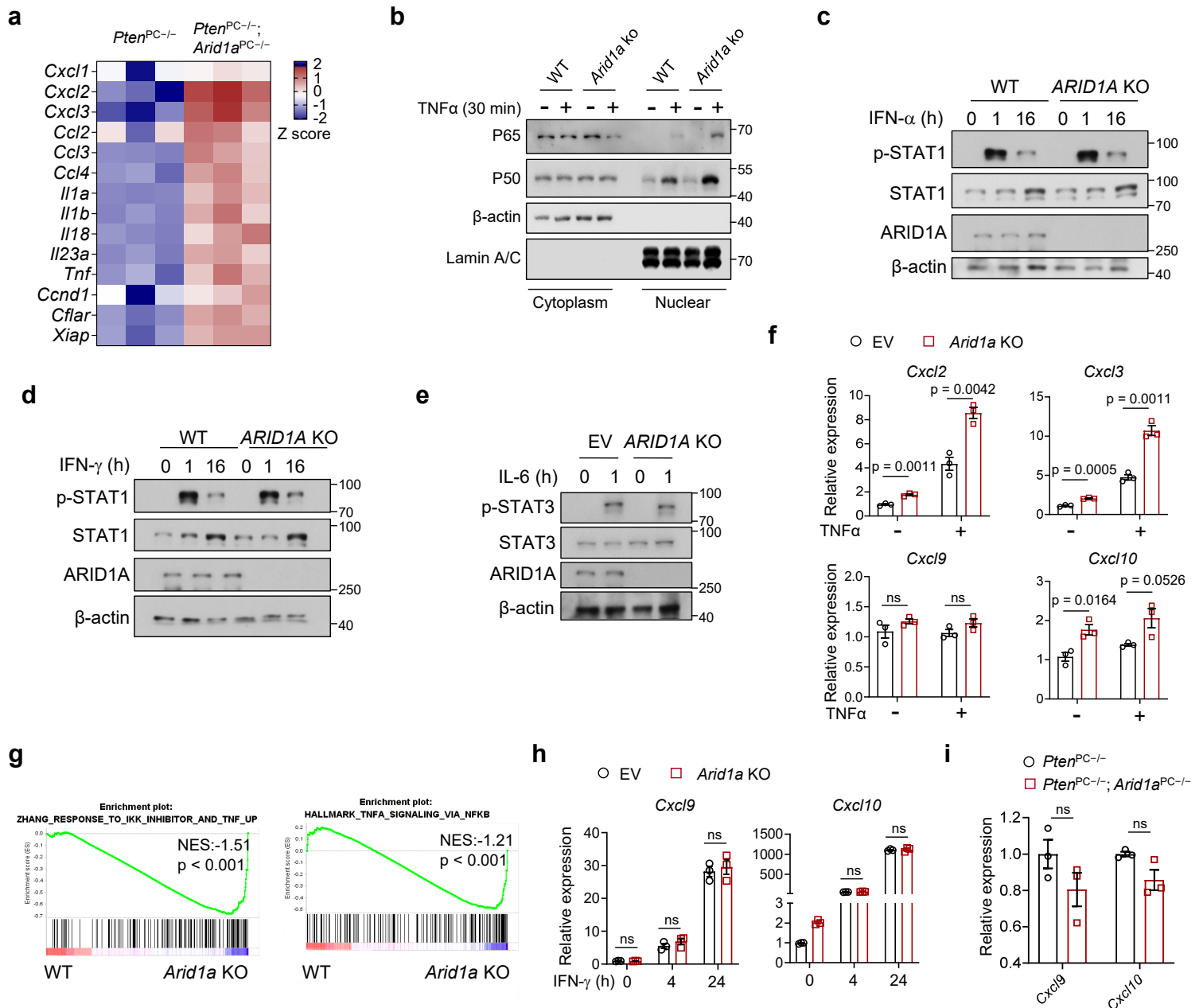




Supplementary Figure 2. PMN-MDSC enrichment promotes the progression of *Arid1a*-deleted tumors.

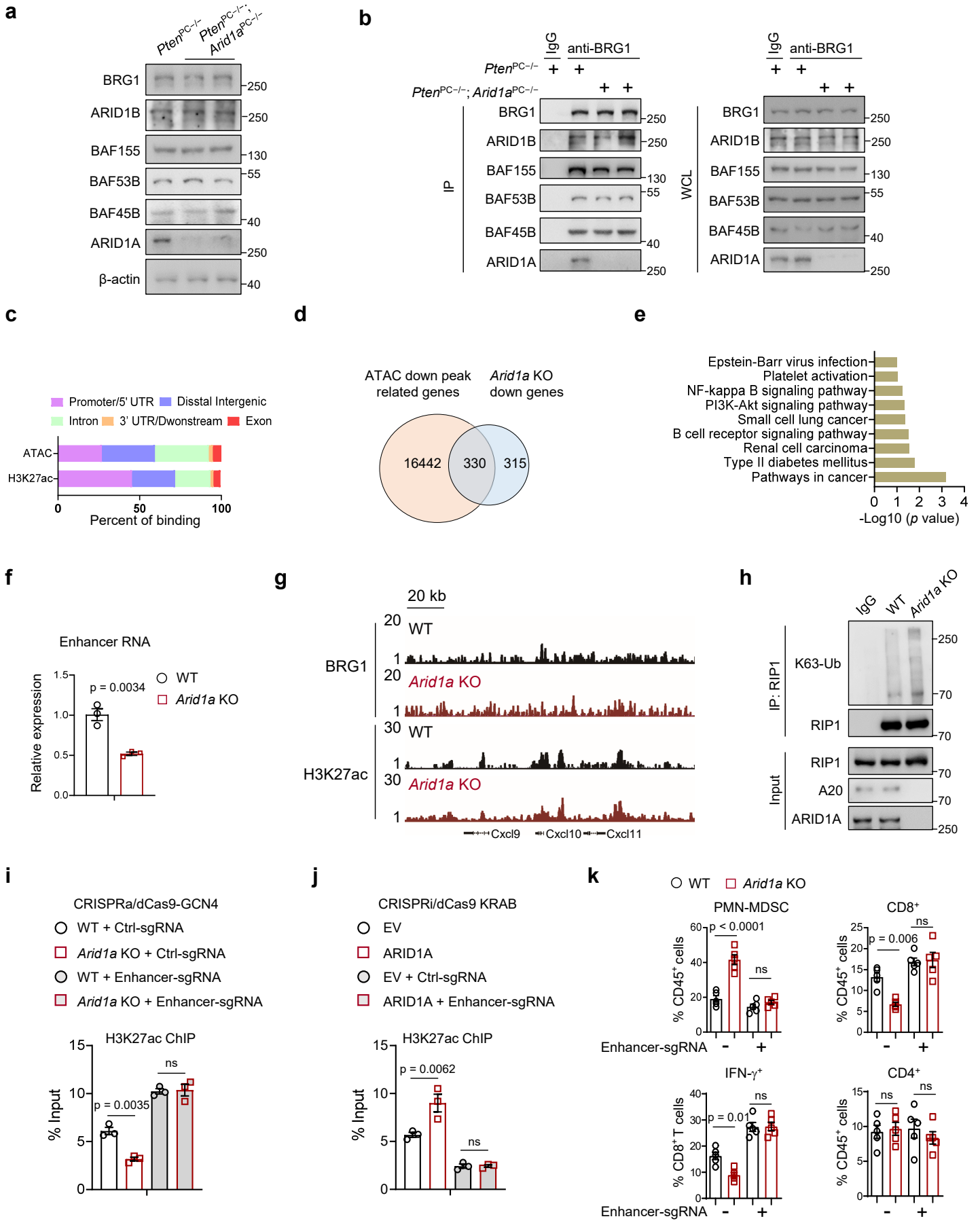
a, Percentage of CD45⁺ immune cells in 3-month-old *Pten*^{PC-/-} and *Pten*^{PC-/-}; *Arid1a*^{PC-/-} prostate tumors (n = 8). **b**, Gating strategy for FACS analysis (Fig. 2c) is shown for tumor-infiltrating immune cells. The same strategy was used for the subsequent experiments. **c**, qRT-PCR analysis of Ly6G⁺ cells from 3-month-old *Pten*^{PC-/-}; *Arid1a*^{PC-/-} prostate tumors and peripheral blood of WT mice (n = 5). *p* values for the individual gene expression in Ly6G⁺ cells of peripheral blood and tumor: *Nos2* ($p < 0.0001$), *Nox2* ($p = 0.0004$), *Arg1* ($p = 0.0017$), *S100a9* ($p = 0.0019$), *Stat3* ($p < 0.0001$), *Cxcl10* ($p = 0.0001$), *Cxcl4* ($p < 0.0001$), *Tnf* ($p = 0.0001$), *Il6* ($p < 0.0001$), *Ccl9* ($p = 0.0001$). **d**, Summary of T cell proliferation assessed by CFSE flow cytometry after 4 days of co-culture. High and low proliferation were defined as T cell division ≥ 2 and ≤ 1 , respectively (n = 5). **e**, IFN- γ secretion by CD8⁺ T cells measured by ELISA (n = 5). **f**, Representative images of organoids and quantification as indicated (n = 10 fields from 3 experiments per group). Scale bar, 500 μ m. **g**, Volume of subcutaneous tumors derived from WT and *Arid1a* KO Myc-CaP cells with or without anti-Ly6G antibody treatment. WT + Isotype, WT + anti-Ly6G or *Arid1a* KO + anti-Ly6G (n = 12, each group); *Arid1a* KO + Isotype (n = 11). **h**, Quantification of tumor-infiltrating immune cells in WT and *Arid1a* KO Myc-CaP subcutaneous tumors with or without anti-Ly6G antibody treatment (n = 6). **i**, The prostate weights of *Pten*^{PC-/-}; *Arid1a*^{PC-/-} mice with or without anti-Ly6G administration. The treatment was performed twice a week for 4 weeks when the mice were 10-week-old (n = 6). **j**, Quantification of Ki67⁺ and CD8⁺ in prostate sections. **k**, Flow cytometry analysis of PMN-MDSCs, CD8⁺ T cells and IFN γ ⁺ CD8⁺ T cells (n = 6). **l**, Graphical scheme describing the ADT strategy. **m**, Gross photographs and volume of prostates from the indicated mice with ADT (n = 10). Scale bar, 1 cm. *p* value for the prostatic volume: AP ($p < 0.0001$), DLP ($p < 0.0001$) and VP ($p < 0.0001$). **n**, H&E-stained sections in 5-month-old *Pten*^{PC-/-} and *Pten*^{PC-/-}; *Arid1a*^{PC-/-} prostates after ADT (n = 10, representative data are shown). Scale bars, 50 μ m. **o**, Quantification of histological grade from the indicated mice with ADT (n = 10). **p**, Immunohistochemical analysis in castrated prostate sections. Scale bar, 50 μ m.

a, **c**, **e-k**, **m**, Data represent the mean \pm SEM. Statistical significance was determined by two-tailed unpaired *t* test (**a**, **c**, **e**, **i-k**, **m**), Fisher's exact test (**d**), one-way ANOVA followed by multiple comparisons (**f**), two-way ANOVA followed by multiple comparison (**g**, **h**) and χ^2 test (**o**). **p**, Representative data of triplicate experiments are shown. Source data are provided as a Source Data file. ** $p < 0.01$, ns, no significance.



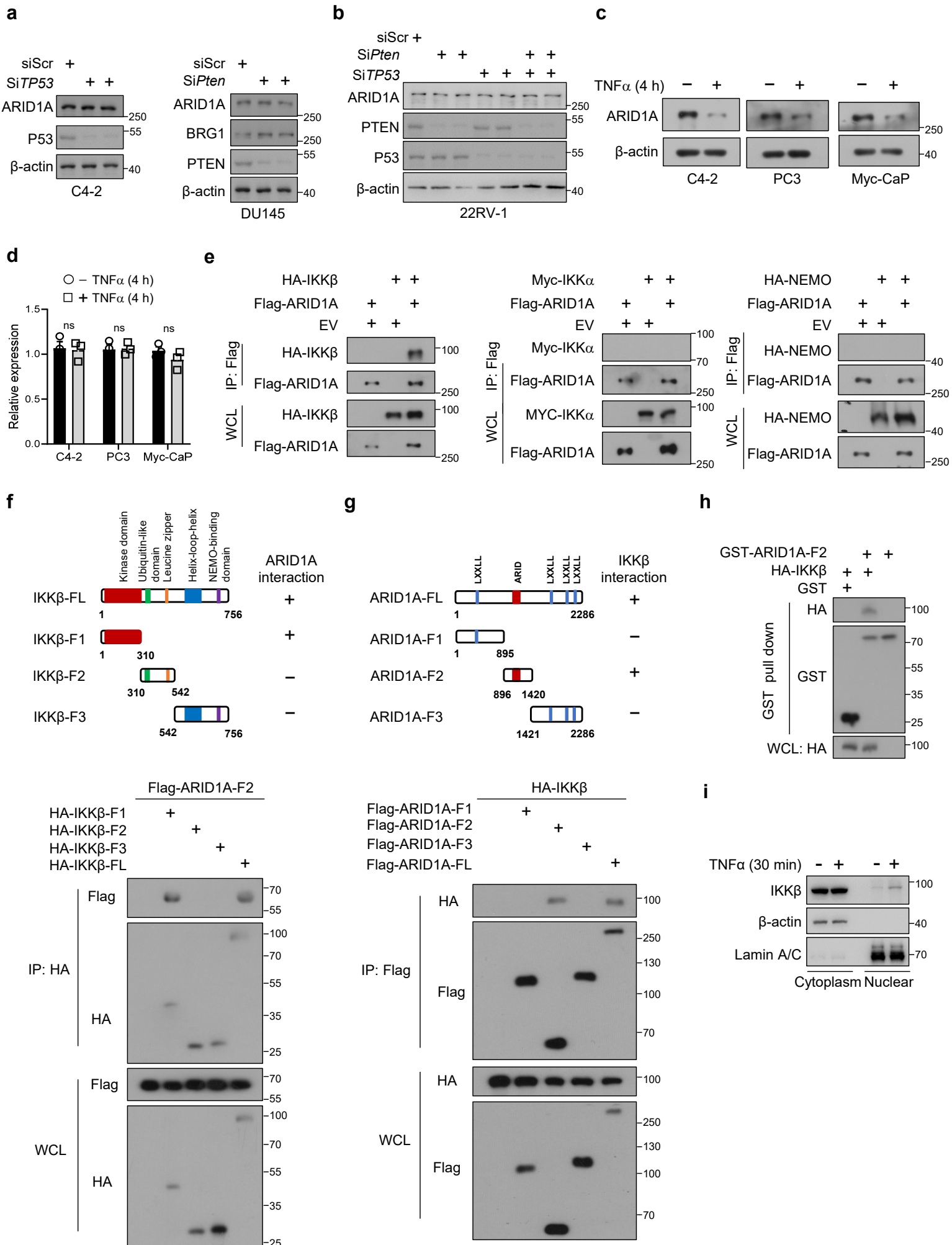
Supplementary Figure 3. ARID1A loss activates NF- κ B signaling to enhance the recruitment of MDSCs.

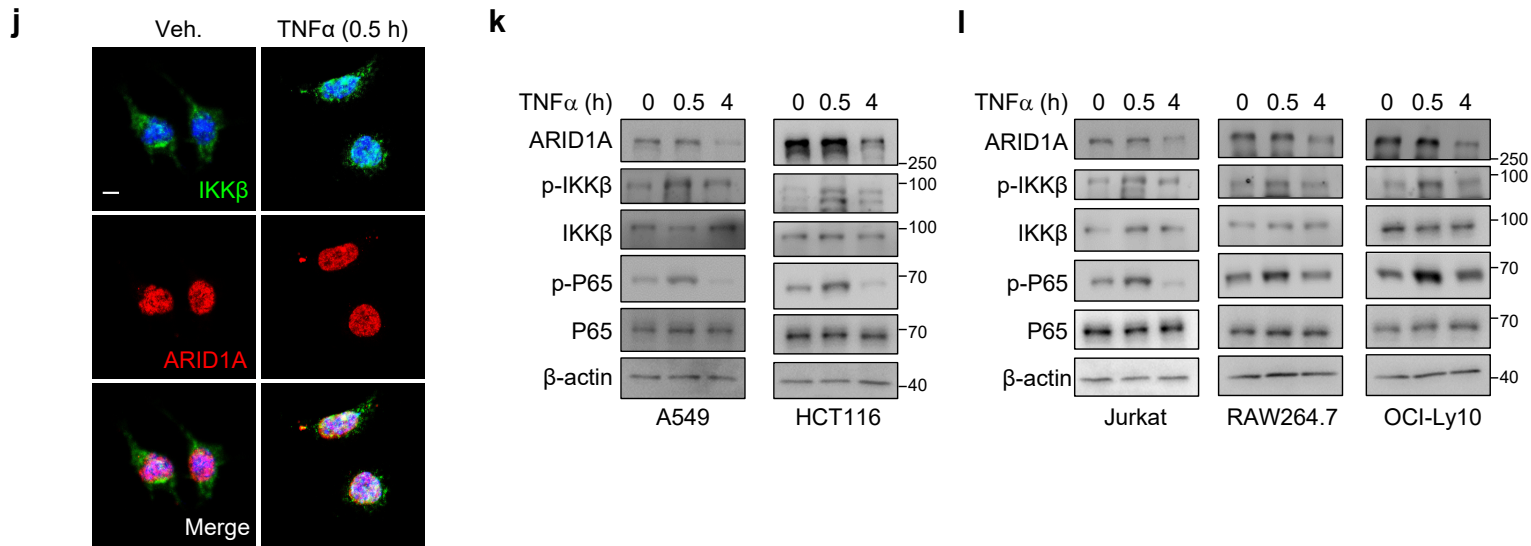
a, Heatmap summarizing the qRT-PCR results in epithelial cells of 3-month-old *Pten*^{PC-/-} and *Pten*^{PC-/-}; *Arid1a*^{PC-/-} mouse prostates (n = 3). **b**, IB analysis of the indicated proteins in cytoplasmic extracts and nuclear extracts from Myc-CaP cells stimulated with TNF α (30 min). **c-e**, IB analysis of WT and *Arid1a*-KO Myc-CaP cells with or without IFN α (**c**), IFN γ (**d**) and IL-6 (**e**) stimulation. **f**, The qRT-PCR results in WT and *Arid1a* KO Myc-CaP cells with or without TNF α stimulation (n = 3). **g**, Hyperactivation of NF- κ B in *Arid1a*-depleted Myc-CaP cells analyzed by GSEA. NES, normalized enrichment score. *p* value was determined by GSEA. **h**, *Cxcl9* and *Cxcl10* transcripts were quantified by real-time PCR in sg*Arid1a*- and vector-expressing Myc-CaP cells stimulated with IFN γ at the indicated time points (n = 3). **i**, *Cxcl9* and *Cxcl10* transcripts were quantified by real-time PCR in epithelial cells of 3-month-old *Pten*^{PC-/-} and *Pten*^{PC-/-}; *Arid1a*^{PC-/-} prostates (n = 3). **f, h, i**, Data represent the mean \pm SEM and statistical significance was determined by two-tailed unpaired *t* test. **b-e**, Data were evaluated in triplicate, and representative data are shown. Unprocessed immunoblots are shown as source data. ns, no significance.



Supplementary Figure 4. *Arid1a* ablation silences the enhancer of the *A20* gene to stimulate NF- κ B signaling.

a, IB analysis of the indicated protein in 3-month-old *Pten*^{PC-/-} and *Pten*^{PC-/-}; *Arid1a*^{PC-/-} mouse prostates. **b**, IB analysis of the whole-cell lysate (WCL) from 12-week-old *Pten*^{PC-/-} and *Pten*^{PC-/-}; *Arid1a*^{PC-/-} prostates and anti-BRG1 immunoprecipitates as indicated. **c**, Bar charts revealing the distributions of ATAC-seq peaks and H3K27ac ChIP-seq peaks in vector-expressing Myc-CaP cells. **d**, Venn diagram of the genes showing the reduced accessibility and expression simultaneously in *Arid1a* KO Myc-CaP cells compared to WT cells. **e**, GO-BP enrichment of the overlapped 85 genes by DAVID, ranked according to *p* value. **f**, *A20* enhancer RNA were quantified by real-time PCR (n = 3). **g**, ChIP-seq tracks of BRG1 and H3K27ac signals in *Cxcl9*, *Cxcl10* and *Cxcl11* gene loci, as indicated. **h**, IB analyses of the WCL and anti-RIP1 immunoprecipitates of Myc-CaP cells. Cells were treated with 20 ng/ml TNF α for 30 min before harvesting. **i**, ChIP-qPCR assays of H3K27ac at the *A20* enhancer in WT and *Arid1a* KO Myc-CaP cells with or without *A20* enhancer activation (CRISPRa/dCas9-based induction, n = 3). **j**, ChIP-qPCR assays of H3K27ac at the *A20* enhancer in WT and ARID1A overexpressing Myc-CaP cells with or without *A20* enhancer silencing (CRISPRi/dCas9-based suppression, n = 3). **k**, Quantification of tumor-infiltrating immune cells in WT and *Arid1a* KO tumors with or without *A20* enhancer activation by FACS (n = 5). **f, i-k**, Data represent the mean \pm SEM and statistical significance was determined by two-tailed unpaired *t* test. **a, b, h**, Experiments were repeated three times independently with similar results; data from one representative experiment are shown. Source data are provided as a Source Data file. ns, no significance.

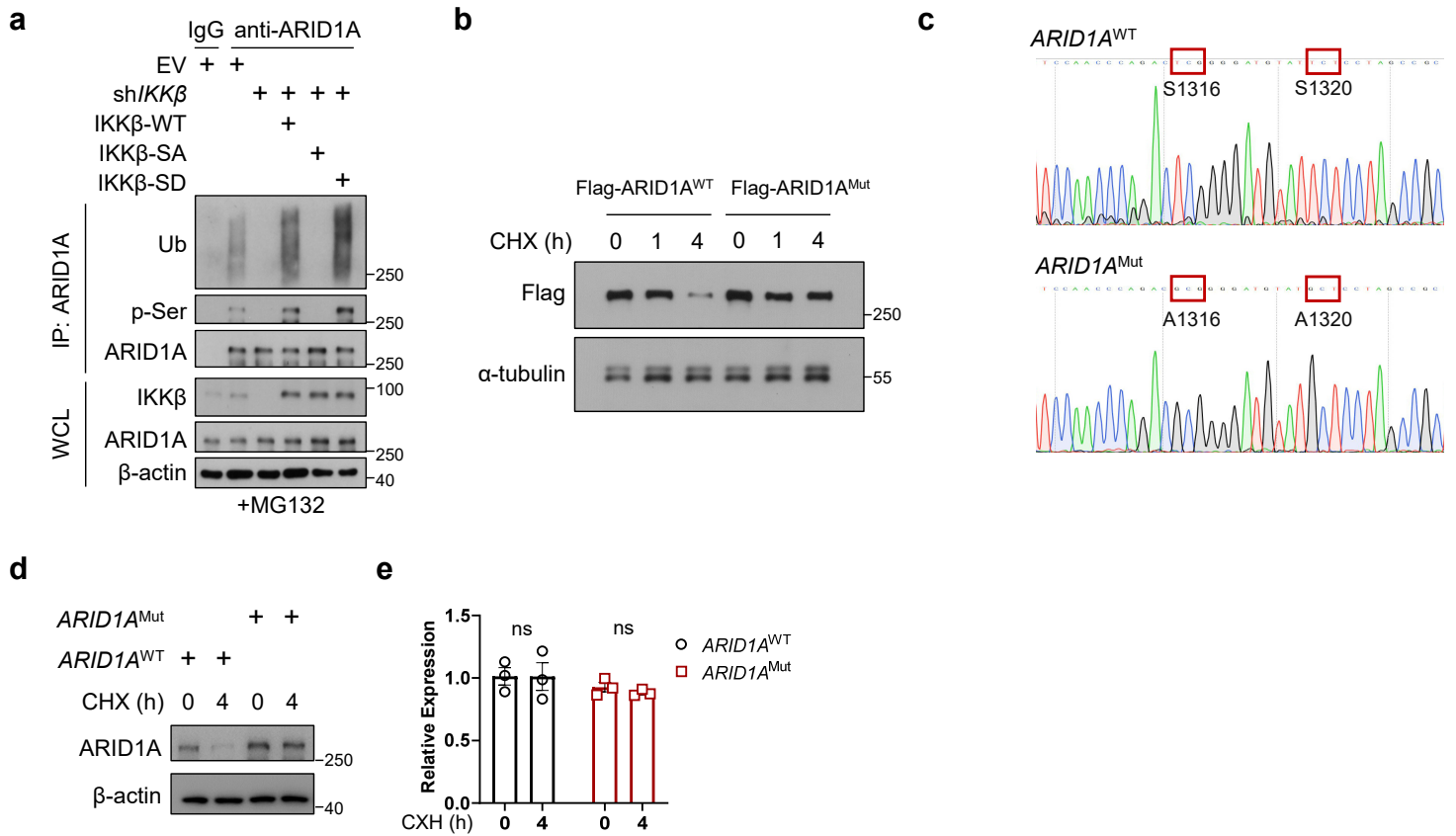




Supplementary Figure 5. IKK β promotes ARID1A reduction in PCa cells.

a, IB analysis of C4-2 and DU145 cells with *TP53* or *Pten* KD, respectively. **b**, IB analysis of 22RV-1 cells with *TP53* an/or *Pten* KD. **c**, IB analysis of C4-2, PC3 and Myc-CaP cells treated with TNF α for the indicated duration of time. **d**, *ARID1A* transcripts were quantified by real-time PCR in PCa cells with or without TNF α stimulation (n = 3), ns, no significance. **e**, IB analysis of the indicated protein in the WCL and immunoprecipitates from 293T cells transfected with Flag-ARID1A and HA-IKK β , Myc-IKK α or HA-NEMO. **f**, Interaction between ARID1A and IKK β . Flag-ARID1A-F2 and HA-IKK β full-length (IKK β -FL) and mutants (IKK β -F1, IKK β -F2, IKK β -F3) were ectopically expressed in 293T cells, followed by anti-HA immunoprecipitation and immunoblotting with Flag and HA antibodies. **g**, HA-IKK β and Flag-ARID1A full-length (ARID1A-FL) and mutants (ARID1A-F1, ARID1A-F2, ARID1A-F3) were ectopically expressed in 293T cells, followed by anti-Flag immunoprecipitation and immunoblotting. **h**, In vitro binding of ARID1A-F2 to IKK β by GST pulldown analysis. **i**, IB analysis of the indicated proteins in cytoplasmic extracts and nuclear extracts from Myc-CaP cells stimulated with TNF α . **j**, IKK β and ARID1A immunostaining as indicated in Myc-CaP cells. Scale bar, 100 μ m. **k**, IB analysis of A549 and HCT116 cells treated with TNF α for the indicated duration of time. **l**, IB analysis of Jurkat, RAW264.7 and OCI-Ly10 cells treated with TNF α for the indicated duration of time.

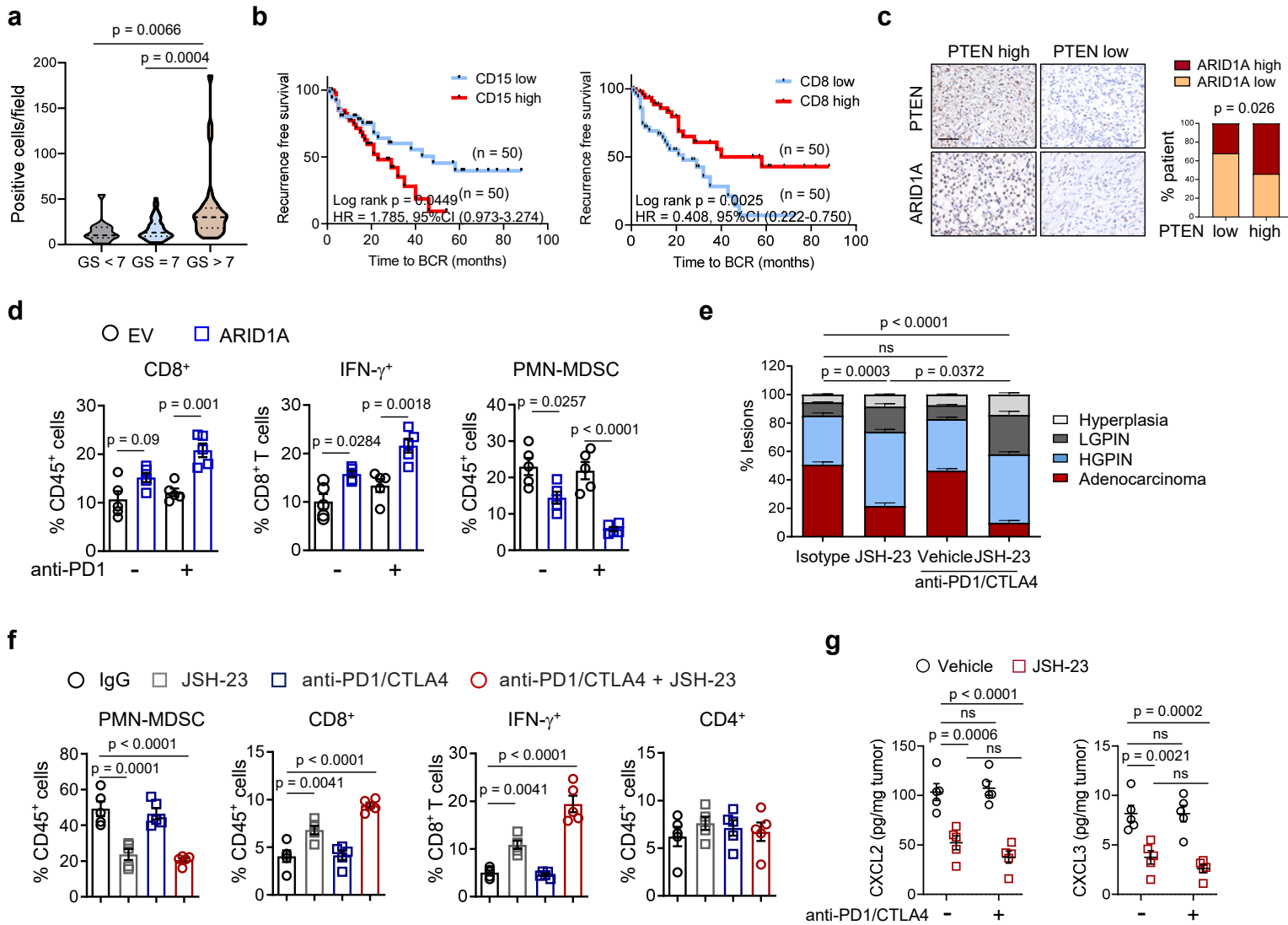
d, Data represent the mean \pm SEM and statistical significance was determined by two-tailed unpaired *t* test. All experiments were repeated three times independently with similar results; data from one representative experiment are shown. Source data are provided as a Source Data file.



Supplementary Figure 6. IKKβ phosphorylates ARID1A and promotes its β-TRCP-dependent degradation.

a, IB analysis of the WCL and immunoprecipitates of the indicated proteins in C4-2 control and *IKKβ* KD cells with or without *IKKβ*-WT, *IKKβ*-SA or *IKKβ*-SD overexpression. **b**, IB analysis of 293T cells with WT or mutant *ARID1A* overexpression treated with TNFα for the indicated duration of time. **c**, Sequencing validations of the CRISPR *ARID1A*-SA knock-in allele in C4-2 cells. **d**, IB analysis of WT and *Arid1a*^{mut} Myc-CaP cells with or without CHX treatment for the indicated duration of time. **e**, *Arid1a* transcripts were quantified by real-time PCR. ns, no significance.

e, Data represent the mean ± SEM and statistical significance was determined by two-tailed unpaired *t* test. **a**, **b**, **d**, Experiments were repeated three times independently with similar results; data from one representative experiment are shown. Source data are provided as a Source Data file.



Supplementary Figure 7. Targeting ARID1A or its coordinated signals increase the sensitivity to ICB therapy.

a, CD15 expression levels stratified by GS in TMA (GS < 7, $n = 14$, GS = 7, $n = 53$, GS > 7, $n = 33$). **b**, Kaplan-Meier plot of recurrence after radical prostatectomy based on the proportions of CD15⁺ and CD8⁺ cells in patients ($n = 50$ for each group). **c**, IHC analysis for ARID1A and PTEN. Scale bars, 50 μ m. The correlation between PTEN and ARID1A expression is shown as stacked columns ($n = 100$). **d**, Quantification of each tumor-infiltrating immune cell population in WT and ARID1A-overexpressing Myc-CaP xenografts with or without anti-PD-1 treatment ($n = 5$). **e**, Prostate tumor histology of *Pten*^{PC-/-}; *Arid1a*^{PC-/-} mice with or without NF- κ B inhibition (JSH-23) in combination with anti-PD1/CTLA-4 treatment ($n = 10$). **f**, Quantification of the indicated tumor-infiltrating immune cell population of *Pten*^{PC-/-}; *Arid1a*^{PC-/-} mouse prostates with or without JSH-23 treatment in combination with anti-PD1/CTLA-4 therapy ($n = 5$). **g**, ELISA of CXCL2 and CXCL3 in prostate tumors of 4-month-old *Pten*^{PC-/-}; *Arid1a*^{PC-/-} mice treated as indicated ($n = 5$).

d-g, Data represent the mean \pm SEM. Statistical significance was determined by one-way ANOVA followed by multiple comparisons (**a**), log-rank test (**b**), χ^2 test (**c**, **e**) and two-way ANOVA followed by multiple comparisons (**d**, **f**, **g**). Source data are provided as a Source Data file. ns, no significance.

Supplementary Table 1. Clinical Summary of Tissue Microarray from PCa Patients, Related to Figure 1 and Figure 7

Variables	tumor	Benign Prostatic Hyperplasia
Numbers	100	40
Age at diagnosis, yr	50-82 (mean 67.8)	
Year of surgery	2012/8-2020/3	
PSA at diagnosis, ng/ml	0.48-157.9 (mean 25.4)	
Pathologic Gleason score, n (%)		
6	14 (14)	
7	53 (53)	
8	14 (14)	
9	18 (18)	
10	1 (1)	
No. of biochemical recurrence, n (%)	39 (39)	
Adverse pathologic events, n (%)		
Extra-prostatic extension	18 (18)	
Seminal vesicle invasion	15 (15)	
Positive surgical margins	2 (2)	

Supplementary Table 2. Clinical Summary of Tumor Tissue Specimens from Advanced PCa Patients, Related to Figure 7

Variables	Adenocarcinoma
Numbers	42
Age at diagnosis, yr	49-79 (mean 68)
PSA at diagnosis, ng/ml	0.07-359.87 (mean 58.25)
Pathologic Gleason score at initial diagnosis, n (%)	
8	10 (23.8)
9	28 (66.7)
10	4 (9.5)
Samples from body sites, n (%)	Prostate, 42 (100%)

Supplementary Table 3. Oligonucleotides

Oligonucleotides	
siP50-1	CGCCUGAAUUCUUCGUAU
siP50-2	CCAGAGUUUACAUCUGAUG
siP52-1	ACAUUGAGGUUCGGUUCUA
siP52-2	GGACAUGACUGCCCAAUUU
siP65-1	CGGAUUGAGGAGAAACGUA
siP65-2	AUGGAUUCAUUACAGCUUA
siIKK α -1	GCAGAUGACGUUUGGUAUA
siIKK α -2	UAGGGUCUGGGAUUCGAUA
siIKK β -1	CCAGCCAAGAAGAGUGAAG
siIKK β -2	GCUGGUUCAUAUCUUGAAC
siNEMO-1	GAGGGAGUACAGCAAACUG
siNEMO-2	GCUCGAUCUGAAGAGGCAG
siPTEN-1	GCAGAUAAUGACAAGGAUUAUUA
siPTEN-2	GGUGAAGAUUAUUCUCCAUA
siTRP53-1	GGAGTATTTGGATGACAG
siTRP53-2	AACCUCUUGGUGAACCUUAGUAC
Primers for shRNA	
ARID1A-shRNA-homo-1	F:CCGGGCTGTGCAGTAGAGTGTAGACTCGAGTCTACACTCTACTGCACAGGCTTTTTG R:AATTCAAAAAGCCTGTGCAGTAGAGTGTAGACTCGAGTCTACACTCTACTGCACAGGC
ARID1A-shRNA-homo-2	F:CCGGGCTGCCACGTGTGTATATACTCGAGTATATACACACGTGGCAGCTTTTTG R:AATTCAAAAAGCTGCCACGTGTGTATATACTCGAGTATATACACACGTGGCAGC
ARID1A-shRNA-homo-3	F:CCGGGCGAGACACAGCTATTTAATCCTCGAGGATTAATAGCTGTGTCTCGCTTTTTG R:AATTCAAAAAGCGAGACACAGCTATTTAATCCTCGAGGATTAATAGCTGTGTCTCGC
IKK β -shRNA-homo-1	F:CCGGGCTGATTGTGTGTGTGAAACACTCGAGTGTTCACACACACAATCAGCTTTTTG R:AATTCAAAAAGCTGATTGTGTGTGTGAAACACTCGAGTGTTCACACACACAATCAGC
IKK β -shRNA-homo-2	F:CCGGGGACAGTGTCCAATTCAAATCCTCGAGGATTTGAATTGGACACTGTCTTTTTG R:AATTCAAAAAGGACAGTGTCCAATTCAAATCCTCGAGGATTTGAATTGGACACTGTCC
IKK β -shRNA-homo-3	F:CCGGGGATTGAGCTTCTCCTAAACACTCGAGTGTAGGAGAAGCTGAATCCTTTTTG R:AATTCAAAAAGGATTGAGCTTCTCCTAAACACTCGAGTGTAGGAGAAGCTGAATCC
Arid1a-shRNA-mus-1	F:CCGGCAGGCCCTATGGCCCTAATATCTCGAGATATTAGGGCCATAGGGCCTGTTTTG R:AATTCAAAAACAGGCCCTATGGCCCTAATATCTCGAGATATTAGGGCCATAGGGCCTG
Arid1a-shRNA-mus-2	F:CCGGTGCCCAAGATCGAGGTTATATCTCGAGATATAACCTCGATCTTGGGCATTTTTG R:AATTCAAAAATGCCCAAGATCGAGGTTATATCTCGAGATATAACCTCGATCTTGGGCA
Primers for real-time RT-qPCR	
A20-mus	F:ACTGGAATGACGAATGGGACA R:CAGGGAATTGACTGAAGTCCAC
Cxcl1-mus	F:ACTGCACCCAAACCGAAGTC R:TGGGGACACCTTTTAGCATCTT
Cxcl2-mus	F:CCAACCACCAGGCTACAGG R:GCGTCACACTCAAGCTCTG
Cxcl3-mus	F:GATTTTGAGACCATCCAGAGC R:CTCTTCAGTATCTTCTTGATG
Cxcl9-mus	F:GGAGTTCGAGGAACCCTAGTG R:GGGATTTGTAGTGGATCGTGC
Cxcl10-mus	F:CAAAGTGTCTGCCGTCATTTTC R:GGCTCGCAGGGATGATTTCAA
Cxcl11-mus	F:GTAACCAGTCAGCCTGAG R:GCTTTCTCCAGGACTCTTG
Ccl2-mus	F:GGCCTGTCTTACAGTTG R:CTGCTGGTGATCCTCTTGTAG
Ccl3-mus	F:CTGCAACCAAGTCTTCTCAG R:GCCGGTTTCTCTTAGTCAGG
Ccl4-mus	F:CTTCTGTGCTCCAGGGTTCTC R:CTGTCTGCCTCTTTGGTCAG
Ccl5-mus	F:GCTGCTTTGCTACCTCTCC R:TCGAGTGACAAACACGACTGC
Arid1a-mus	F:CTTCCCAACACCAGTACAA R:CTGTGCGAAGGACGACAGAC
Arid1b-mus	F:GTTGTATGGGATGGTACTCACC R:CTGGTTGTAGTATGGTGCTG
Ar-mus	F:CTGGGAAGGGTCTACCCAC R:GGTGCTATGTTAGCGGCCTC
Tmprss2-mus	F:CAGTCTGAGCACATCTGTCCT R:CTCGGAGCATACTGAGGCA
Ck8-mus	F:TCCATCAGGGTGACTCAGAAA R:CCAGCTTCAAGGGGCTCAA
Ck18-mus	F:CAGCCAGCGTCTATGCAGG R:CTTTCTCGGTCTGGATTCCAC
Ck5-mus	F:TCTGCCATACCCCATCTGT R:CCTCCGCCAGAAGTGTAGGA
Trp63-mus	F:TACTGCCCCGACCCTTACAT R:GCTGAGGAAGTCTGCTGTCTG
Ezh2-mus	F:AGTGACTTGGATTTTCCAGCAC R:AATTCTGTTGTAAGGGCGACC
Sox2-mus	F:GCGGAGTGGAAACTTTTGTCC R:CGGGAAGCGTGTACTTATCCTT
Ascl1-mus	F:GCAACCGGGTCAAGTTGGT R:GTCGTTGAGTAGTTGGGGG
Brg1-mus	F:CAAAGACAAGCATCTCTAGCCA R:CACGTAGTGTGTGTTAAGGACC
Baf155-mus	F:AGCTAGATTCGGTGCGAGTCT R:CCACCAGTCCAGCTAGTGTTTT
Actl6a-mus	F:GTGTACGGCGGAGATGAAGTT R:GGGAAATCAACCTTAGGGCAGT
Actl6b-mus	F:GCGCTCGTCTTTGACATTGG R:ATTGGTGTGATGTGGAAAATCT
Brm-mus	F:CTCCTGGACCAATTCTGGGG R:CATCGTTGACAGAGGATGTGAG
Dpf1-mus	F:GAGGCCATCGAGCACTGTC R:CGGGCGGGTAAGTGTAGA
β -actin-mus	F:GGCTGTATCCCCTCCATCG R:CCAGTTGGTAACAATGCCATGT
ARID1A-homo	F:CCTGAAGAAGTCCGACGGGAA R:TCCGCCATGTTGTTGGTGG
Primers for sgRNA	
Arid1a-sgRNA-mus-1	F:CACCGGCAGCTGCGAAGATATCGGG R:AAACCCCGATATCTTCGAGCTGCC
Arid1a-sgRNA-mus-2	F:CACCGTTCGGTAAAGATCGTGAG R:AAACCTGCACGATCTTACCAGGAA
Primers for real-time Chip-qPCR	
A20-mus	F:CAAATCCCTCTACTTACAATCCC R:ACCGAAATCACCTCTGTATGTT
Primers for enhancer RNA	
A20-eRNA-mus	F:TGGCAGGCATTCAGACTACAAA R:AGAGCTTAAAGCAGGGTAGCAAA